# Dynamical Processes related to viscous flow in a supercooled arsenic selenide glass-forming liquid: Results from high-temperature $^{77}$Se NMR Spectroscopy

**[1]Weidi Zhu, [2]Ivan Hung, [2]Zhehong Gan, [3]Bruce Aitken, [1]Sabyasachi Sen***

[1]Department of Materials Science & Engineering, University of California at Davis,

Davis, CA 95616, USA

[2]Center of Interdisciplinary Magnetic Resonance, National High Magnetic Field Laboratory,

1800 East Paul Dirac Drive, Tallahassee, FL 32310, USA

*[3]Science & Technology Division, Corning Inc., Corning, NY 14831, USA*

**corresponding author (email: sbsen@ucdavis.edu)*

## Abstract

Dynamical processes in supercooled $AsSe_9$ liquid are studied using 1D and 2D $^{77}Se$ NMR spectroscopic techniques. The results demonstrate the coexistence of two distinct dynamical processes: one is a slow process related to the chemical exchange between the various Se environments by bond scission/renewal and the other is the fast Se chain segmental motion, which leads to the rapid averaging of the chemical shift anisotropy. The timescales of these two processes become increasingly similar as the glass transition is approached from above. The slow process is found to be closely coupled to viscosity over the entire temperature range of investigation and its activation energy is consistent with the Se-Se/As bond energies. On the other hand, the activation energy of the fast process is significantly higher, which may be indicative of its cooperative nature. This process becomes coupled to viscosity only in the immediate vicinity of the glass transition.

## 1. Introduction

The structural relaxation processes near the glass transition region are key in controlling the technological utility of glasses and glass-ceramics. For example, glass products retain thermal stress caused by quenching, which decreases the strength and durability of the product and needs to be removed after forming via annealing [1]. This stress removal proceeds with structural relaxation at temperatures close to the glass transition via processes that are closely related to the viscous flow with an identical activation energy. On the other hand, for glass-ceramic processing, the crystallization is controlled by self-diffusion which is inversely proportional to the viscosity, as predicted by the Stokes-Einstein equation. These relaxation processes have been treated in the literature principally as macroscopic phenomena within the framework of phenomenological models [2-5]. However, a direct mechanistic understanding of the structural relaxation process at the atomic scale often remains lacking.

Previous dynamical studies of supercooled oxide network liquids have suggested a close mechanistic association between the local bond-breaking and reforming of the network and viscous flow. For example, high-temperature $^{29}$Si, $^{11}$B, $^{17}$O, $^{31}$P and $^{27}$Al NMR spectroscopic studies have shown that in borate, silicate and phosphate liquids the average time scale of the local Si-O, B-O or P-O bond breaking and chemical exchange between Si or P atoms belonging to different Q-species or between B atoms in $BO_3$ and $BO_4$ species correspond well with the shear relaxation time scale derived from viscosity data [6-12]. The flow mechanism appears to be facilitated by the ability of oxygens to reconfigure between bridging and non-bridging arrangements, with corresponding changes in silicon, phosphorus or boron configurations. It may be noted here that, although these studies were the first of their kind for high temperature oxide liquids and they provided a tremendous wealth of structural and dynamical information, they have

so far been primarily restricted to 3-dimensional oxide networks. On the other hand, little is known regarding the structural relaxation mechanisms in chalcogenide liquids, characterized by networks with a wide range of connectivity and topological characteristics. For example, Se or S rich chalcogenide liquids are characterized by low-dimensional polymer-like networks of sparsely cross-linked Se and S chains, while over some composition ranges the structure of these liquids may be dominated by molecular units [13-17]. Increasing addition of Ge or As, on the other hand, results in predominantly corner-shared tetrahedral or pyramidal networks. The viscous flow mechanism in these liquids at the atomic scale remains poorly known to date.

Raman spectroscopic studies of structural changes accompanying aging in Ge-Se and Si-Se glasses and *in situ* high-temperature Raman spectroscopy of a $GeSe_4$ supercooled liquid have indicated temperature dependent conversion between the edge- and corner-sharing $GeSe_{4/2}$ or $SiSe_{4/2}$ tetrahedra via Ge-Se or Si-Se bond scission and rearrangement [18,19]. The timescales of such processes were reported to be consistent with that of shear relaxation. On the other hand, high-temperature $^{31}P$ and $^{77}Se$ NMR spectroscopic studies of the speciation equilibria and chemical exchange kinetics in P-Se liquids were carried out by Eckert and coworkers [20-22]. These studies have revealed two important aspects of the dynamical processes in these topologically complex networks. First of all, similar to oxide liquids, P atoms are chemically exchanged between the $P_4Se_3$ molecules and the surrounding P-Se-P network via P-Se bond scission and renewal. Second, the orientational averaging of the $^{31}P$ chemical shift anisotropy (CSA) of the molecular and network P sites occurs at a rate that is significantly faster than that of chemical exchange, presumably via fast rotation of the molecular units and network segments of $PSe_{3/2}$ pyramidal units linked by short Se-Se chain moieties. When taken together, these results indicate the presence of two distinct dynamical modes, consistent with the nature of the topological elements in these

liquids. However, the relative contributions of these two processes to shear relaxation in these liquids remains poorly understood. Recent shear relaxation measurements on supercooled chalcogenide liquids have also indicated the presence of two distinct dynamical processes in Se-rich As-Se and Ge-Se liquids [23]. The slow process was reported to be coupled to viscous flow at all temperatures, while the fast process becomes a major contributor to viscosity only near the glass transition [24]. Here we report the results of a high-temperature 1D and 2D $^{77}$Se NMR spectroscopic study of the $AsSe_9$ supercooled liquid near its glass transition to reveal the atomistic nature of these dynamical processes. The relative coupling of these processes to viscous flow and shear relaxation are shown to be crucial in understanding the nature of the glass transition of chalcogenide liquids.

## 2. Experimental

### *2.1. Sample synthesis*

The $AsSe_9$ glass was synthesized from the constituent elements (≥99.999% purity, metal basis) that were melted in an evacuated ($10^{-6}$ Torr) and flame sealed fused silica ampoule (8 mm I.D., 12 mm O.D.) in a rocking furnace at 650°C for 24 hours. Finally, the melt was quenched to glass by dipping the ampoule in water.

### *2.2. High-temperature static 1D $^{77}$Se NMR*

The high-temperature static $^{77}$Se NMR spectra of the supercooled $AsSe_9$ liquid were acquired using a Bruker Avance500 spectrometer operating at 11.74 T ($^{77}$Se Larmor frequency 95.4 MHz) and a Bruker wideline probe. Crushed glass was packed and flame-sealed in an evacuated Pyrex ampoule and heated using nitrogen gas. Temperature of the probe was calibrated externally using

the well-known temperature dependence of the $^{63}$Cu chemical shift of CuBr [25]. A Hahn echo pulse sequence ($\pi/2-\tau-\pi-$acquisition) was employed for spectral acquisition with $\pi/2$ pulse length of 3.5 μs and $\tau$ = 63 μs. The recycle delay was varied from a maximum of 60 s at room temperature and near the highest temperature of ~ 500K to a minimum of 5 s near 430 K. Each spectrum was obtained by Fourier transforming the average of 1024 free induction decays.

*2.2. Static 2D $^{77}$Se Exchange Spectroscopy (EXSY)*

2D EXSY ($\pi/2-t_1-\pi/2-t_{mix}-\pi/2-$acquisition) spectra were acquired at the National High Magnetic Field Laboratory in Tallahassee, Florida on a Bruker Avance NEO console operating at a $^{77}$Se Larmor frequency of 114.4 MHz ($B_0$ = 14.1 T, $\nu_0(^1H)$ = 600 MHz). Experiments were performed with a static HX Low-E probe designed and built at the NHMFL, which has a horizontal 5 mm solenoidal detection coil. Crushed glass powder was packed in a Bruker 4 mm $ZrO_2$ rotor. Each 2D spectrum was acquired with a total of 32 hypercomplex $t_1$ data points, 128 to 512 transients per point depending on the mixing time ($t_{mix}$), and 3 μs $\pi/2$-pulses. Recycle delays of 3 and 10 s were used at T = 358 and 348 K, respectively. Temperature was controlled to within ±0.1 K, for the entire duration of the experiment. The $^{77}$Se NMR spectra were referenced to neat $(CH_3)_2Se$ with $\delta_{iso}$ = 0 ppm by using the $^{17}$O signal of $H_2O$ and the frequency ratios listed for $^{17}$O and $^{77}$Se in the IUPAC recommendations [26].

## 3. Results and Discussion

The temperature dependent evolution of the 1D $^{77}$Se NMR line shape of $AsSe_9$ supercooled liquid at temperatures ranging between 405 and 499 K is shown in Fig. 1. The $^{77}$Se NMR spectrum at 405 K is characterized by 3 resolved resonances centered at 900, 840 and 650 ppm. Following

previous high-resolution $^{77}$Se NMR studies of $As_xSe_{1-x}$ glasses, and taking the well-known temperature dependence of $^{77}$Se chemical shifts in chalcogenides into account, the resonance at 900 ppm corresponds to Se-**Se**-Se sites with Se next-nearest neighbors, while the one at 840 ppm corresponds to Se-**Se**-Se sites with one or more As next-nearest neighbors [27-29]. The resonance at ~ 650 ppm, on the other hand, can be assigned to Se-**Se**-As sites [27,28]. It is important to note here that the $^{77}$Se NMR line shape near 400 K provides significant enhancement in resolution compared to the ambient-temperature $^{77}$Se NMR spectra of $As_xSe_{1-x}$ glasses [28]. The $^{77}$Se spectral line shapes at low temperatures are known to be severely broadened by both the CSA as well as the chemical shift distribution resulting from the structural disorder in glasses. The increased spectral resolution at high temperatures near 400 K implies motional averaging of these broadening effects. Further increase in temperature beyond ~ 400 K shows clear evidence for initial chemical exchange induced broadening and subsequent collapse of the $^{77}$Se NMR line shape into a symmetric peak in the motionally narrowed regime (Fig. 1). It is intuitively obvious that such chemical exchange between different Se environments in the liquid can only occur via Se-Se and Se-As bond scission/renewal dynamics. The timescale for this process can then be estimated by simulating the high-temperature $^{77}$Se NMR line shapes in Fig. 1 using a dynamical model of chemical exchange. Here we use a random three-site chemical exchange model, where exchange between any pair of Se environments is equally probable and, thus, all exchange events characterized by the same timescale. The analytic expression for the resulting line shape is given by [30] the real part of $g(\omega)$, where $g(\omega) = \frac{1}{N}\frac{L}{1-(L/\tau_{NMR})}$ and $L = \sum_{j=1,N}\left[i(\omega-\omega_j) + \frac{1}{T_{2j}} + N/\tau_{NMR}\right]^{-1}$. In these expressions N is the total number of sites, $\omega_j$ is the frequency and $T_{2j}$ is the reciprocal of the intrinsic linewidth corresponding to each site, and $(\tau_{NMR})^{-1} = R_{ex}$ is the rate of

chemical exchange between the different sites. The value of $T_{2j}$ has been kept constant at 1 ms for all sites in all of the simulations and only $R_{ex}$ is varied as a function of temperature. The shift in the positions of the $^{77}$Se resonances due to thermal expansion can be significant, but is known from previous studies and has also been incorporated into all the simulations [29]. It is clear from Fig. 1 that this simple model of the chemical exchange dynamics is able to reproduce the experimental $^{77}$Se NMR line shapes quite well. On the other hand, the motional averaging of the CSA and chemical shift distribution induced broadening effects for the –Se-**Se**-Se– resonance reaches a maximum at ~ 385 K (Fig. 2). Such an averaging may come from rotational reorientation of these selenium environments, resulting, for example, from the segmental motion of the -Se-Se-Se- chain elements in the structure. Previous $^{77}$Se NMR isotropic-anisotropic shift correlation spectroscopic studies reported that the broadening effects for the –Se-**Se**-Se– resonance from both CSA and chemical shift distribution are similar in magnitude, ~ 150 ppm (Fig. 2) [27]. Therefore, the timescale $\tau_f$ for the segmental chain rotation responsible for the averaging of the –Se-**Se**-Se– line broadening at ~ 385K is on the order of the inverse of the linewidth, i.e., $\tau_f \sim 7\times10^{-5}$ s.

These dynamical processes can be probed at lower temperatures closer to glass transition ($T_g$ = 344 K) using 2D $^{77}$Se EXSY NMR. The static $^{77}$Se EXSY spectra of the $AsSe_9$ liquid just above $T_g$, at 348 and 358K, are shown in Fig. 3 as a function of the mixing time. While at the shortest mixing time the spectral intensity is localized along the diagonal, it is clear that the Se-**Se**-Se and Se-**Se**-As resonances broaden individually as the intensity for each Se environment starts to expand off-diagonal with increasing mixing time. At around 100 ms (1000 ms) at 358 K (348 K), the intensity for the –Se-**Se**-Se– site completely loses its diagonal character (Fig. 3). This broadening corresponds to the averaging of the chemical shift interactions resulting from the rotational reorientation of the selenium chain segments in the structure. The characteristic

timescale for this dynamical process is therefore semi-quantitatively determined as $\tau_f \sim 100$ ms and 1000 ms at 358 K and 348 K, respectively (Fig. 3). More precise estimation of the timescales requires direct simulation of these spectra, which remains prohibitively difficult due to the lack of constraints on the relative broadening effects of the static line shapes from the distributions of the isotropic and anisotropic chemical shift. Further increase in the mixing time results in a significant development of cross-peak intensities associated with chemical exchange between the two basic types of Se environments. However, due to the abovementioned difficulty with direct simulation, an estimation of the timescale for the chemical exchange dynamics from the growth rate of the cross-peak intensity is not attempted in this work. Finally, it is interesting to note that the EXSY spectra are somewhat asymmetric about the diagonal, especially at 358K, with significantly higher intensity in the lower right quadrant that is stretched out along the *f2* dimension (Fig. 3). Such asymmetry most likely results from the fact that the recycle delay of 3s used at 358K may not be sufficient for complete relaxation of both selenium environments (see below) and that the spin-lattice relaxation rate of the Se-**Se**-Se resonance is faster than that of the Se-**Se**-As resonance [31]. However, further systematic studies are required to test this hypothesis.

When taken together, the 1D and 2D $^{77}$Se NMR spectroscopic results reveal two important aspects of the dynamical processes in these topologically complex networks. First of all, similar to oxide liquids, the bond scission/renewal dynamics and chemical exchange between Se environments must play an important role in controlling the mass and momentum transport (i.e., diffusivity and viscosity, respectively) in this Se-rich As-Se liquid. Second, and in contrast with the case of oxide liquids, the orientational averaging of the $^{77}$Se CSA of the Se-**Se**-Se and Se-**Se**-As sites is complete at lower temperatures. The timescale of the dynamical process responsible for this averaging is therefore significantly faster than that of chemical exchange. A similar

observation was also made in a previous high-temperature $^{77}$Se wideline NMR study on binary As-Se supercooled liquids by Rosenhahn et al. [28].

The presence of two distinct dynamical modes is consistent with the coexistence of rather different types of topological elements in these liquids, namely, the selenium chains and the $AsSe_{3/2}$ pyramids. Fast rotation and/or segmental motion of the chain units can average the $^{77}$Se CSA and chemical shift distribution, while the slow Se/As-Se bond breaking and chemical exchange between the selenium environments control the collapse of the high-temperature line shape. The assignment of the fast process to segmental chain dynamics also implies that this process must disappear in chalcogenide liquids with progressive cross-linking of selenium chains, e.g., via addition of As or Ge, which leads to the shortening and eventual disappearance of the chain segments. This hypothesis was borne out in recent rheological studies of As-Se and Ge-Se binary liquids [23], where liquids with ≥10-15 atom% Ge or As are indeed characterized by a single relaxation process. The temperature dependence of the relaxation times $\tau_s = \tau_{NMR}$ , for the slow chemical exchange and $\tau_f$ for the fast process, as derived from the NMR results presented in this study, are shown as a function of scaled temperature $T_g$/T in Fig. 4. Here the calorimetric $T_g$ is used for the temperature scaling.

Nuclear spin relaxation is another technique that can provide complementary information of the atomic dynamics including motional correlation times and activation energy. The $^{77}$Se NMR spin-lattice relaxation data were collected under non-spinning condition as a function of temperature, using a saturation recovery pulse sequence. A comb of sixteen π/2 rf pulses was used to saturate the magnetization and spectra were collected as a function of magnetization recovery delays of up to 10s following the saturation, using a π/2 observation pulse. It may be noted that the low natural abundance of $^{77}$Se and its long relaxation time, combined with the probability of

crystallization above $T_g$, severely limits the temperature range over which the spin-lattice relaxation time $T_1$ could be measured to obtain reliable activation energies. Therefore, we have focused the measurements to obtain a precise location of the $T_1$ minimum for the Se-**Se**-Se resonance, as it directly yields the correlation time $\tau_{SLR}$ at that temperature to be the inverse of the Larmor frequency (Fig. 5). This data point is included in Fig. 4, which clearly indicates that $\tau_{SLR}$ is consistent with $\tau_f$ and, thus, the fast process is likely responsible for the spin-lattice relaxation of $^{77}$Se nuclides in the Se-**Se**-Se chain environments in this system, at least at elevated temperatures.

Although $\tau_s$ and $\tau_f$ are characterized by rather different activation energies, they both reach the value of ~ 100 s near $T_g$ (Fig. 4), which is the expected to be the structural relaxation time at the calorimetric glass transition. The activation energy for $\tau_s$ in the temperature range of our measurements is ~180 kJ/mol, which agrees well with Se-Se and Se-As bond energies and provides further support to the bond scission/renewal scenario for this process. On the other hand, the activation energy of $\tau_f$ is significantly higher and more non-Arrhenius (Fig. 4). Such a non-Arrhenius temperature dependence for $\tau_f$ is possibly indicative of a cooperative nature of the segmental or rotational dynamics of the selenium chain moieties. Our recent rheological study of the viscoelastic relaxation in supercooled liquid Se [24] has suggested that the relative contributions of the slow and the fast processes to the viscosity $\eta$ can be estimated by using a modified Maxwell model: $\eta \approx G_s\tau_s + G_f\tau_f$ , where $G_s$ and $G_f$ correspond to the relaxation moduli for the slow and fast processes, respectively. Furthermore, it was shown that $G_s$ can be obtained from creep measurements, as it is simply the reciprocal of the recoverable creep compliance $J_s$ , while $G_f$ is the high-frequency "glassy" modulus, which is on the order of ~ 5 GPa for the $AsSe_9$ composition [32]. The $J_s(T)$ for the supercooled $AsSe_9$ liquid used in the present analysis has been taken from the previous work of Bernatz et al. [33]. The calculated contributions from

the slow process $\eta_s = G_s\tau_s$ and the fast process $\eta_f = G_f\tau_f$ are compared with the experimental viscosity of the $AsSe_9$ liquid in Fig. 6. Clearly, $\eta$(T) is consistent with $\eta_s$(T) over the entire temperature range where experimental data are available for $\tau_s$ (Fig. 6). In contrast, the contribution to viscosity from the fast process is negligible at higher temperatures (Fig. 6). However, it becomes increasingly significant with lowering of temperature and eventually becomes almost identical to the contribution from the slow process as $T_g$ is approached from above (Fig. 6). The increased temporal coupling between the slow and the fast processes with decreasing temperature near $T_g$ is unusual (Fig. 3) in the sense that typically the faster processes in glass-forming liquids get serially decoupled from the slower ones as temperature is lowered. The fundamental origin of such intriguing behavior in $AsSe_9$ liquid remains unclear but it agrees with a similar observation made for supercooled liquid selenium in recent rheological studies [24]. It is important to note here that in the high-temperature limit the timescale of all atomic dynamics should converge to the phonon time (picoseconds) [34]. Therefore, it is likely that $\tau_s$ and $\tau_f$ would converge again at high temperatures.

## 4. Summary

In summary, high-temperature $^{77}$Se NMR spectroscopic results indicate the coexistence of two distinct dynamical processes in $AsSe_9$ liquid. The slow process is related to the chemical exchange between different Se environments via Se-Se and As-Se bond scission/renewal. The fast process, on the other hand, is related to the Se chain segmental motion, which results in the dynamical averaging of the $^{77}$Se chemical shift distribution as well as the CSA at elevated temperatures. The timescales of the two processes become increasingly similar as $T_g$ is approached from above. The viscosity contributions from the two processes are estimated using the Maxwell relation. The slow process is coupled to viscosity over the entire measured temperature range, while the contribution

from the fast process becomes appreciable only near $T_g$. The physical significance of the unusual temperature-dependent temporal coupling between the two processes remain unclear at this stage.

**Acknowledgments**

This work was supported by the National Science Foundation Grant NSF-DMR 1855176 to SS. The National High Magnetic Field Laboratory is supported by National Science Foundation through NSF/DMR-1644779, and the State of Florida.

**References:**


1. Q. Zheng and J. C. Mauro, "Variability in the relaxation behavior of glass: Impact of thermal history fluctuations and fragility", Journal of Chemical Physics, 146, 074504/1-8 (2017).
2. J. C. Dyre, "Colloquium: The glass transition and elastic models of glass-forming liquids", Reviews of Modern Physics, 78, 953-972 (2006).
3. M. D. Ediger, "Spatially heterogeneous dynamics in supercooled liquids", Annual Review of Physical Chemistry, 51, 99-128 (2000).
4. C. A. Angell, K. L. Ngai, G. B. McKenna, P. F. McMillan and S. W. Martin, "Relaxation in glassforming liquids and amorphous solids", Journal of Applied Physics, 88, 3113-3157 (2000).
5. K. Ngai. Relaxation and diffusion in complex systems (Springer, New York, 2011).
6. I. Farnan and J. F. Stebbins, "The nature of the glass transition in a silica-rich oxide melt", Science, 265, 1206-1209 (1994).
7. J.F. Stebbins, S. Sen and I. Farnan, "Silicate species exchange, viscosity, and crystallization in a low-silica melt: In situ high-temperature MAS NMR spectroscopy", American Mineralogist, 80, 861-864 (1995).
8. J.F. Stebbins and S. Sen, in: 2nd International Conf. On Borate Glasses, Crystlas and Melts, ed: A. Wright, S. Feller and A. Hannon, (Society of Glass Technology, Sheffield, UK, 1997).
9. J.F. Stebbins, in: Modern Methods in Solid-state NMR: A Practitioner's Guide, ed: P. Hodgkinson, (Royal Society of Chemistry, 2018).
10. S. Wegner, L. Van Wüllen, G. Tricot, Network Dynamics and Species Exchange Processes in Aluminophosphate Glasses: An in Situ High Temperature Magic Angle Spinning NMR View, J. Phys. Chem. B. 113 (2009) 416–425.
11. L. Van Wüllen, S. Wegner, G. Tricot, Structural Changes above the Glass Transition and Crystallization in Aluminophosphate Glasses: An in Situ High-Temperature MAS NMR Study, J. Phys. Chem. B. 111 (2007) 7529–7534.
12. L. Muñoz-Senovilla, S. Venkatachalam, F. Muñoz, L. Van Wüllen, Relationships Between Fragility and Structure Through Viscosity and High Temperature NMR Measurements in $Li_2O$-ZnO-$P_2O_5$ Phosphate Glasses, J. Non. Cryst. Solids. 428 (2015) 54–61.
13. G. Yang, B. Bureau, T. Rouxel, Y. Gueguen, O. Gulbiten, C. Roiland, E. Soignard, J. L. Yarger, J. Troles, J.-C. Sangleboeuf and P. Lucas, "Correlation between structure and physical properties of chalcogenide glasses in the $As_xSe_{1-x}$ system", Physical Review B, 82/1-8, (2010).
14. T. G. Edwards, S. Sen and E. L. Gjersing, "A combined $^{77}Se$ NMR and Raman spectroscopic study of the structure of $Ge_xSe_{1-x}$ glasses: Towards a self consistent structural model", Journal of Non-Crystalline Solids, 358, 609-614 (2012).
15. S. Soyer-Uzun, S. Sen and B. Aitken, "Network vs molecular structural characteristics of Ge-doped arsenic sulfide glasses: a combined neutron/x-ray diffraction, extended x-ray absorption fine structure, and Raman spectroscopic study", Journal of Physical Chemistry C, 113, 6231-6242 (2009).

16. S. Soyer-Uzun, S. Sen, C. Benmore and B. Aitken, "A combined neutron and X-ray diffraction study of short-and intermediate-range structural characteristics of Ge–As sulfide glasses", Journal of Physics: Condensed Matter, 20, 335105/1-11 (2008).
17. B. G. Aitken, "GeAs sulfide glasses with unusually low network connectivity", Journal of Non-Crystalline Solids, 345, 1-6 (2004).
18. T.G. Edwards and S. Sen, Structure and Relaxation in Germanium Selenide Glasses and Supercooled Liquids: A Raman Spectroscopic Study, J. Phys. Chem. B, 115, 4307-14 (2011).
19. M.A.T. Marple, V. Yong, S. Sen, Fragility and aging behavior of $Si_xSe_{1-x}$ glasses and liquids, J. Chemical Physics, 150, 044506 (2019).
20. R. Maxwell, H. Eckert, Speciation Equilibria, Clustering, and Chemical-Exchange Kinetics in Non-Oxide Glasses and Melts. High-Temperature $^{31}P$ NMR Study of the System Phosphorus-Selenium, J. Am. Chem. Soc. 115 (1993) 4747–4753.
21. R. Maxwell, H. Eckert, Molten-State Kinetics in Glass-Forming Systems. A High-Temperature NMR Study of the System Phosphorus-Selenium, J. Phys. Chem. 99 (1995) 4768–4778.
22. R. Maxwell, H. Erickson, H. Eckert, Depolymerization Kinetics of Glass-Forming Chalcogenide Melts. Coherence Transfer NMR Studies of Phosphorous Selenide, Z. Naturforsch. 50a (1995) 395–404.
23. S. Sen, Y. Xia, W. Zhu, M. Lockhart, B.G. Aitken, Nature of the floppy-to-rigid transition in chalcogenide glass-forming liquids, J. Chemical Physics, 150, 144509 (2019).
24. W. Zhu, B.G. Aitken, S. Sen, Observation of a Dynamical Crossover in the Shear Relaxation Processes in Supercooled Selenium Near the Glass Transition, J. Chem. Phys. 150 (2019) 094502.
25. Hayashi, Shigenobu, and Kikuko Hayamizu. "Nuclear magnetic resonance chemical shifts in alkali iodides, cuprous halides and silver halides." Journal of Physics and Chemistry of Solids 53.2 (1992): 239-248.
26. R. K. Harris, E. D.; De Menezes, S. M. C.; Goodfellow, R.; Granger, P, NMR nomenclature. Nuclear spin properties and conventions for chemical shifts (IUPAC Recommendations 2001), Pure Appl. Chem. 73 (2001) 1795.
27. D.C. Kaseman, I. Hung, Z. Gan, B. Aitken, S. Currie and S. Sen, Structural and Topological Control on Physical Properties of Arsenic Selenide Glasses, Journal of Physical Chemistry B. 118, 2284-2293 (2014).
28. C. Rosenhahn, S.E. Hayes, B. Rosenhahn, H. Eckert, Structural Organization of Arsenic Selenide Liquids: New Results from Liquid State NMR, J. Non. Cryst. Solids. 284 (2001) 1–8.
29. E.L. Gjersing, S. Sen, R.E. Youngman, Mechanistic Understanding of the Effect of Rigidity Percolation on Structural Relaxation in Supercooled Germanium Selenide Liquids, Phys. Rev. B. 82 (2010) 014203.
30. M. Mehring, Principles of High Resolution NMR in Solids, Springer-Verlag, Berlin, 1983.
31. S. Sen, D.C. Kaseman, I Hung, Z. Gan, 77Se Nuclear Spin–Lattice Relaxation in Binary Ge–Se Glasses: Insights into Floppy Versus Rigid Behavior of Structural Units, J. Phys. Chem. B, 119, 5747–5753 (2015).
32. G. Yang, B. Bureau, T. Rouxel, Y. Gueguen, O. Gulbiten, C. Roiland, E. Soignard, J. L.

Yarger, J. Troles, J.-C. Sangleboeuf and P. Lucas, "Correlation between structure and physical properties of chalcogenide glasses in the $As_xSe_{1-x}$ system", Physical Review B, 82/1-8, (2010).
33. K. Bernatz, I. Echeverría, S. Simon and D. Plazek, "Characterization of the molecular structure of amorphous selenium using recoverable creep compliance measurements", Journal of Non-Crystalline Solids, 307, 790-801 (2002).
34. J.C. Dyre, Solidity of viscous liquids. II. Anisotropic flow events, Phys. Rev. E, 59, 7243-7245 (1999).

**Figure captions**

Fig. 1. Experimental (left) and simulated (right) $^{77}$Se static spectral line shape of $AsSe_9$ liquid. Temperatures and corresponding chemical exchange frequencies are denoted alongside each spectrum.

Fig. 2. Comparison between $^{77}$Se NMR isotropic signal for the –Se-**Se**-Se– site in $AsSe_9$ glass at ambient temperature (red line) as reported in [27], and the corresponding $^{77}$Se static line shape for the same site in the supercooled liquid at 385 K (black line). The latter is shifted by 48 ppm to the right for ease of comparison of the linewidth. The full-width-at-half-maximum of the isotropic signal originating entirely from chemical shift distribution is ~ 150 ppm, which is fully averaged to ≤25 ppm in the $^{77}$Se static spectrum.

Fig. 3. Contour plots of 2D $^{77}$Se static EXSY NMR at 358 K (left column) and 348 K (right column) obtained with different mixing times, as listed in each panel. The resonances for the two Se environments are marked with red solid and blue dashed lines on the 1D projection along the F2 dimension (top left) as well as on each contour plot. The diagonals are marked with black dotted lines.

Fig. 4. Timescales for the slow (black symbols) and the fast (red symbols) processes as a function of $T_g$/T. The dashed lines are guides to the eye only.

Fig. 5. $^{77}$Se spin-lattice relaxation time $T_1$ as a function of temperature.

Fig. 6. Contribution to viscosity from the slow (solid black circles) and the fast (open red circles) processes as a function of $T_g$/T. Experimentally measured shear viscosity from literature [31] is shown as open black squares. The dashed lines are guides to the eye only.

**Figure 1**

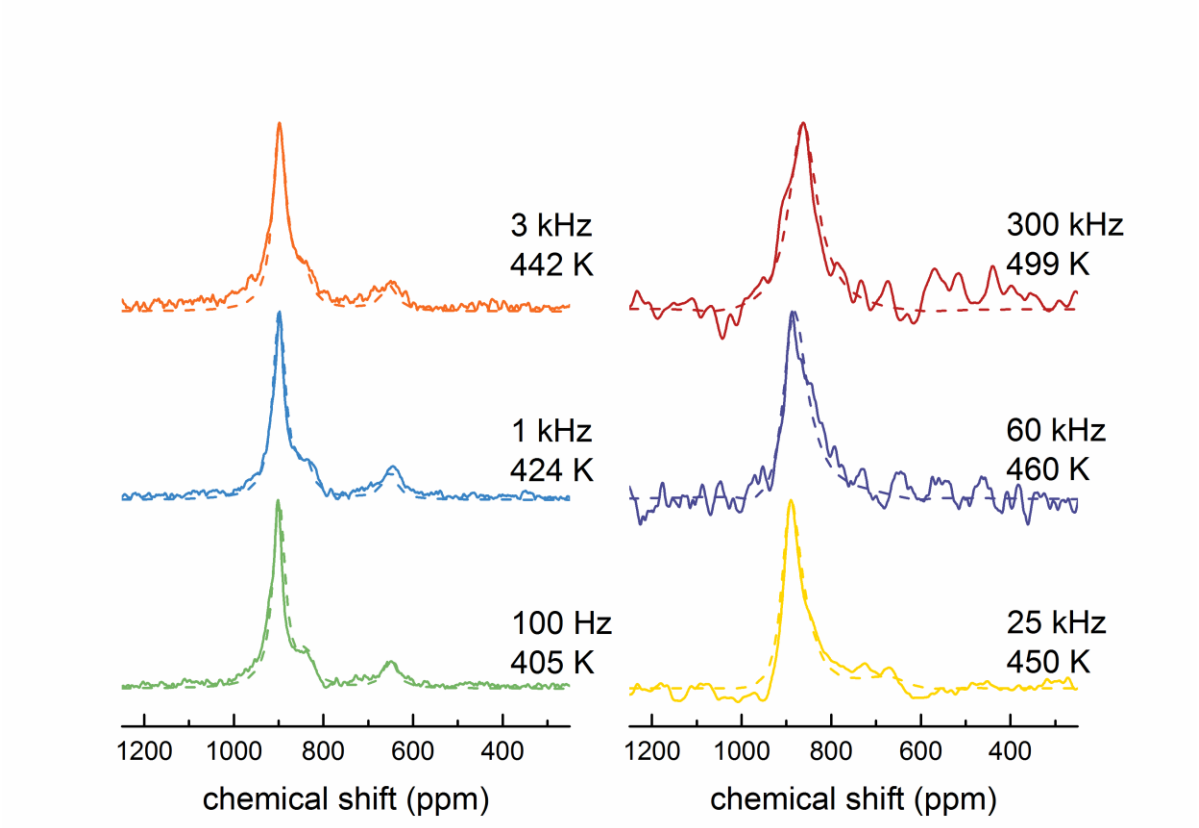
3 kHz
442 K
1 kHz
424 K
100 Hz
405 K
300 kHz
499 K
60 kHz
460 K
25 kHz
450 K
1200
1000
800
600
400
chemical shift (ppm)
1200
1000
800
600
400
chemical shift (ppm)

**Figure 2**

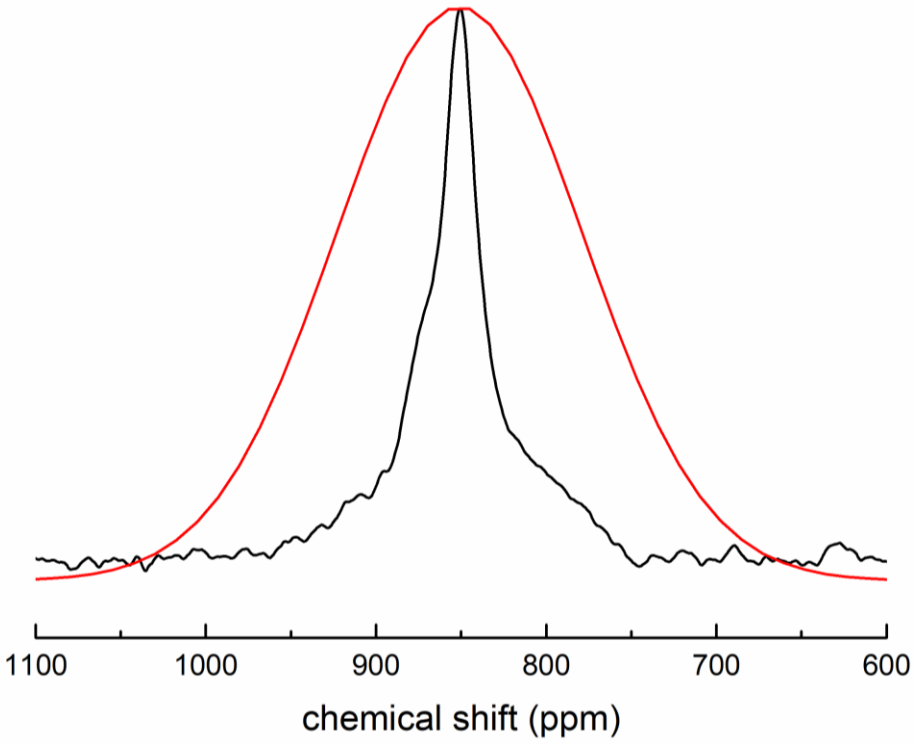

**Figure 3**

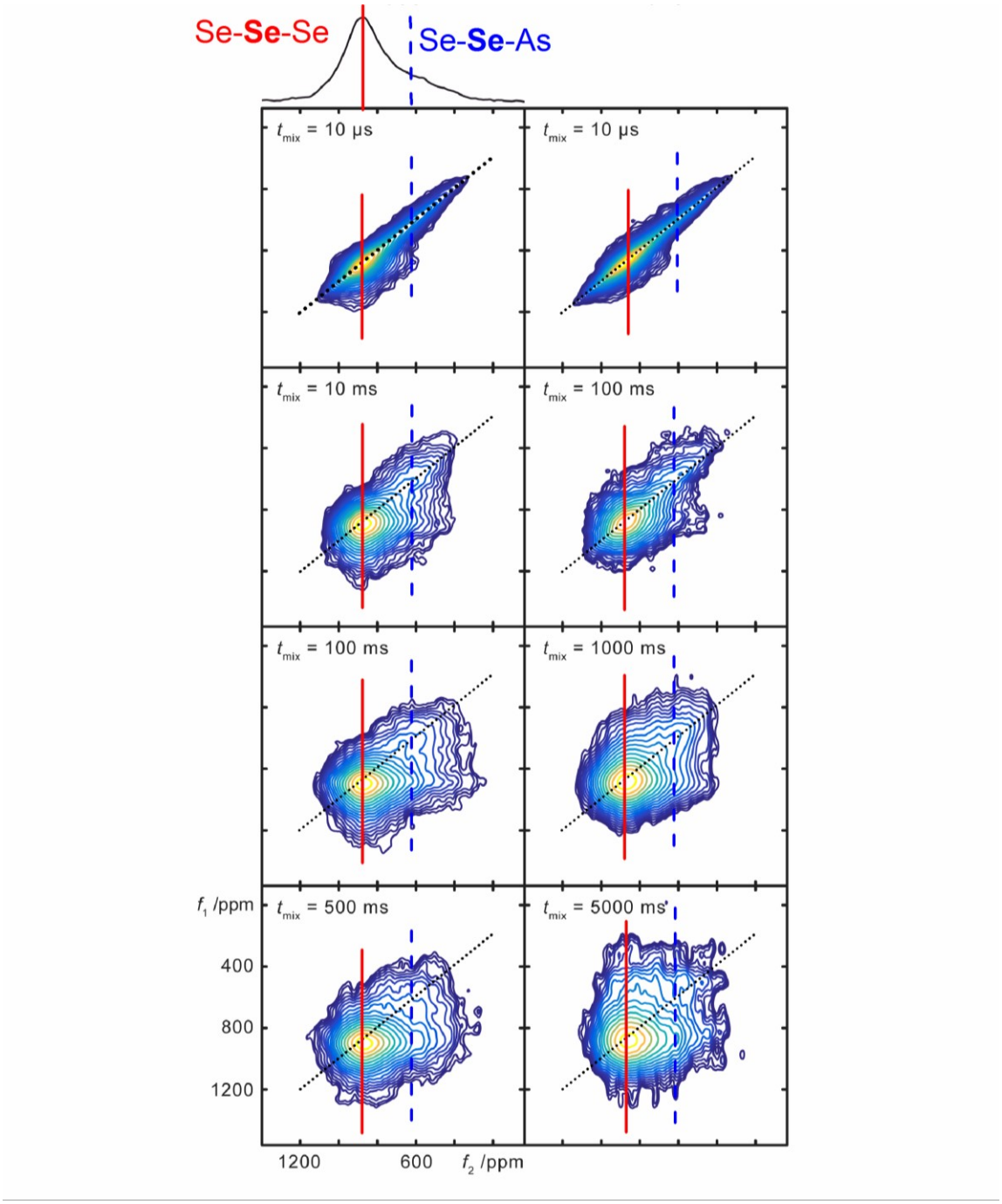
T = 358 K
T = 348 K
Se-Se-Se
Se-Se-As
$t_{mix}$ = 10 µs
$t_{mix}$ = 10 µs
$t_{mix}$ = 10 ms
$t_{mix}$ = 100 ms
$t_{mix}$ = 100 ms
$t_{mix}$ = 1000 ms
$t_{mix}$ = 500 ms
$t_{mix}$ = 5000 ms
$f_1$ /ppm
400
800
1200
1200
600
$f_2$ /ppm

**Figure 4**

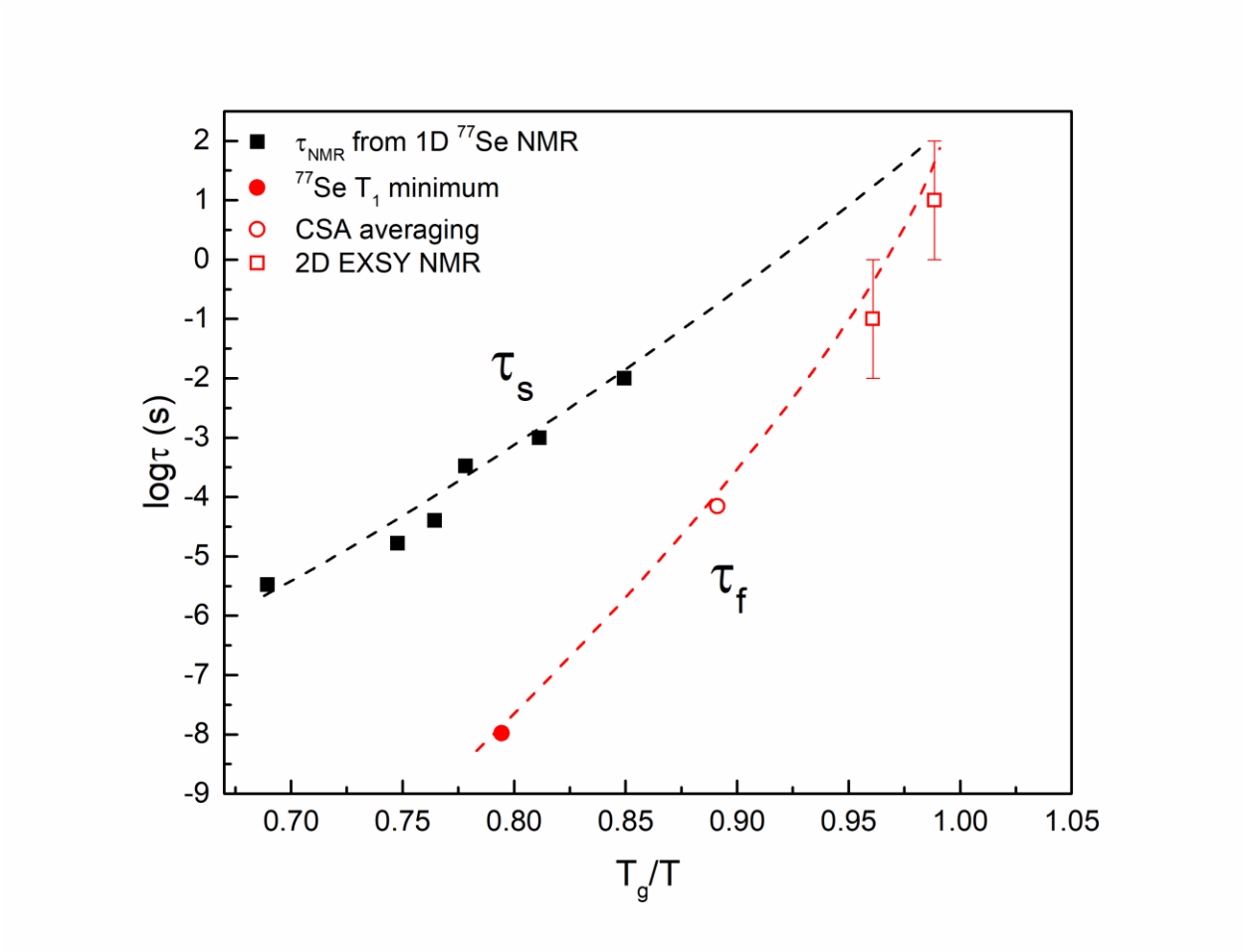
τNMR from 1D 77Se NMR
77Se T1 minimum
CSA averaging
2D EXSY NMR
τs
τf
logτ (s)
Tg/T
2
1
0
-1
-2
-3
-4
-5
-6
-7
-8
-9
0.70
0.75
0.80
0.85
0.90
0.95
1.00
1.05

**Figure 5**

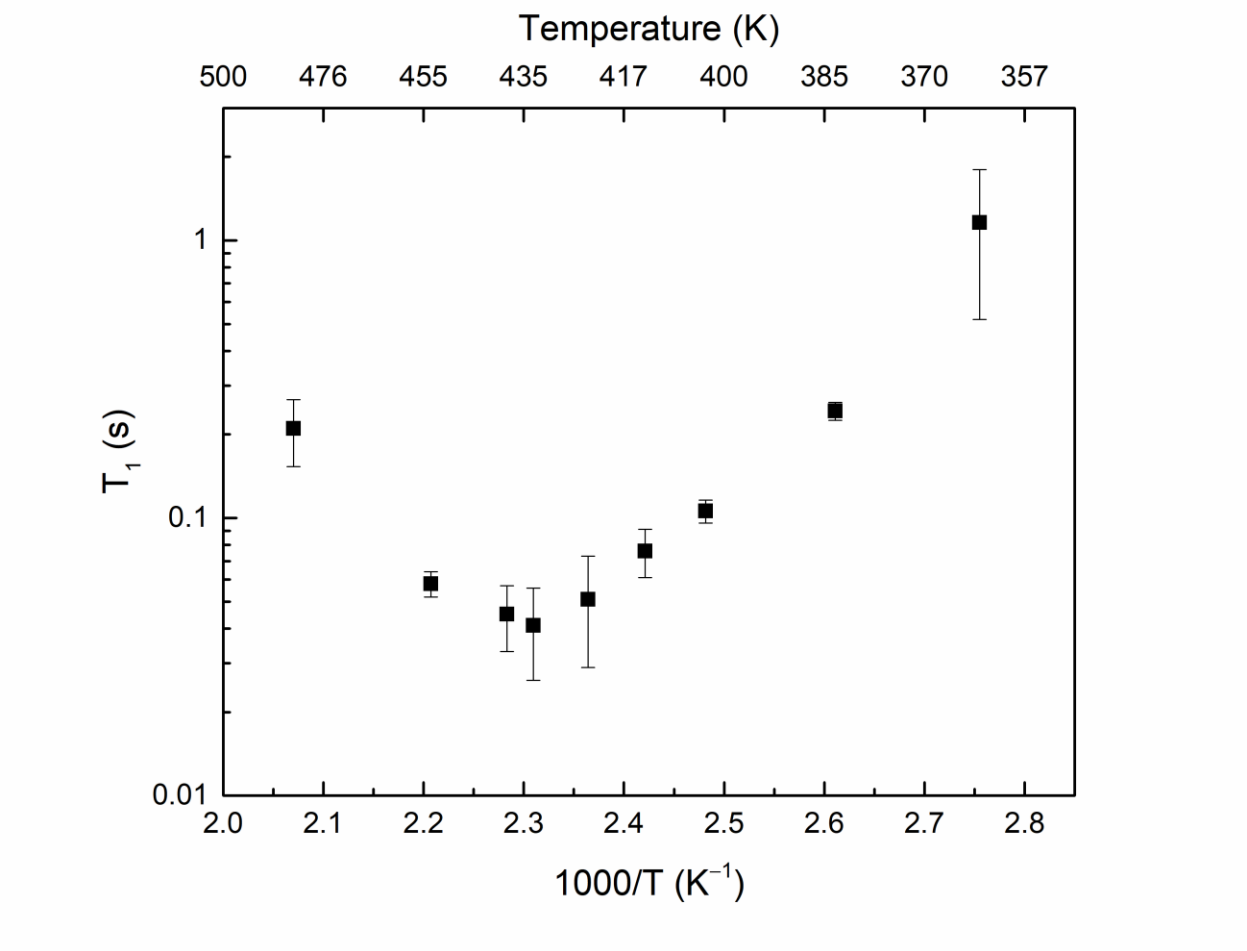
Temperature (K)
500
476
455
435
417
400
385
370
357
1
0.1
0.01
$T_1$ (s)
2.0
2.1
2.2
2.3
2.4
2.5
2.6
2.7
2.8
1000/T ($K^{-1}$)

**Figure 6**

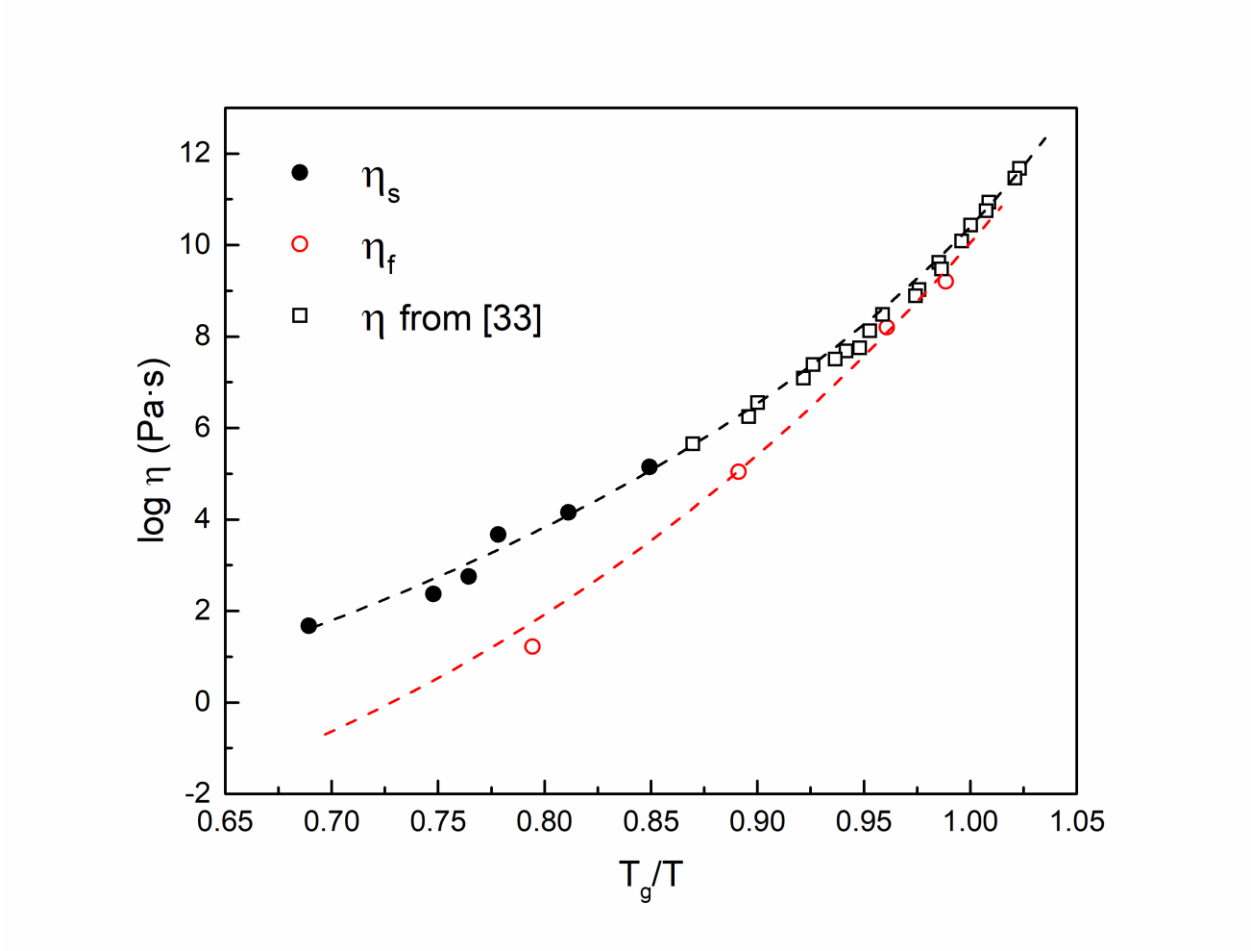
12
10
8
6
4
2
0
-2
log η (Pa·s)
0.65
0.70
0.75
0.80
0.85
0.90
0.95
1.00
1.05
T_g/T
η_s
η_f
η from [33]